



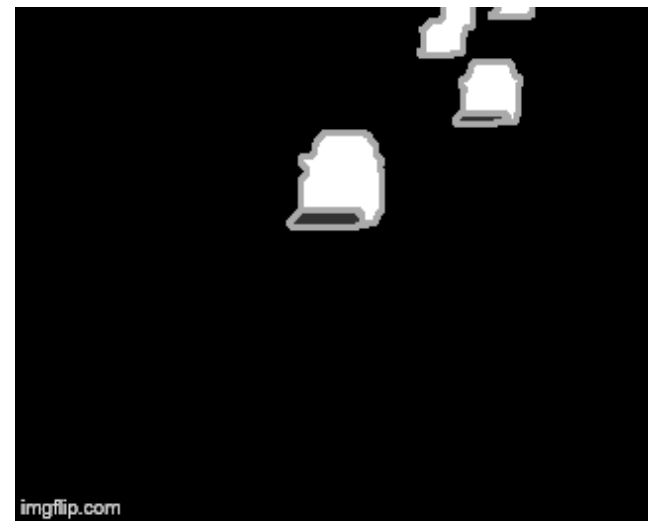
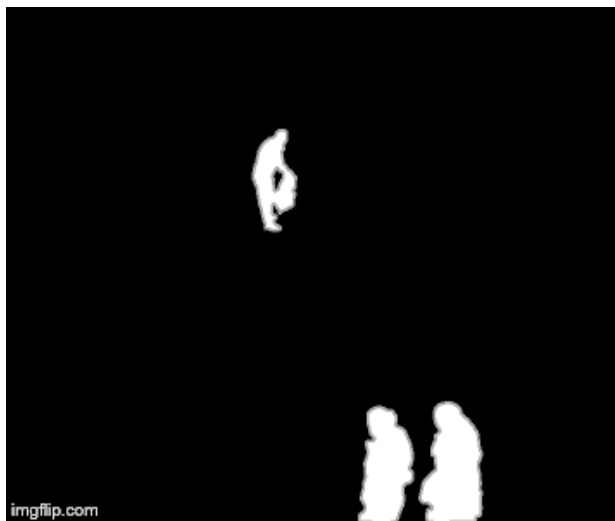
ANTIC: ANTithetic Isomeric Cluster Patterns for Medical Image Retrieval and Change Detection

IET Computer Vision, vol. 13, no. 1, pp. 31-43, 2019

By: Murari Mandal

Introduction: Change Detection

- Motion detection is the fundamental task for many computer vision and video processing applications.
- For example – entertainment industry, healthcare, behavior analysis, traffic monitoring, video segmentation, video synopsis, action recognition, visual surveillance, anomaly detection and object tracking.



System Framework: Moving Object Detection

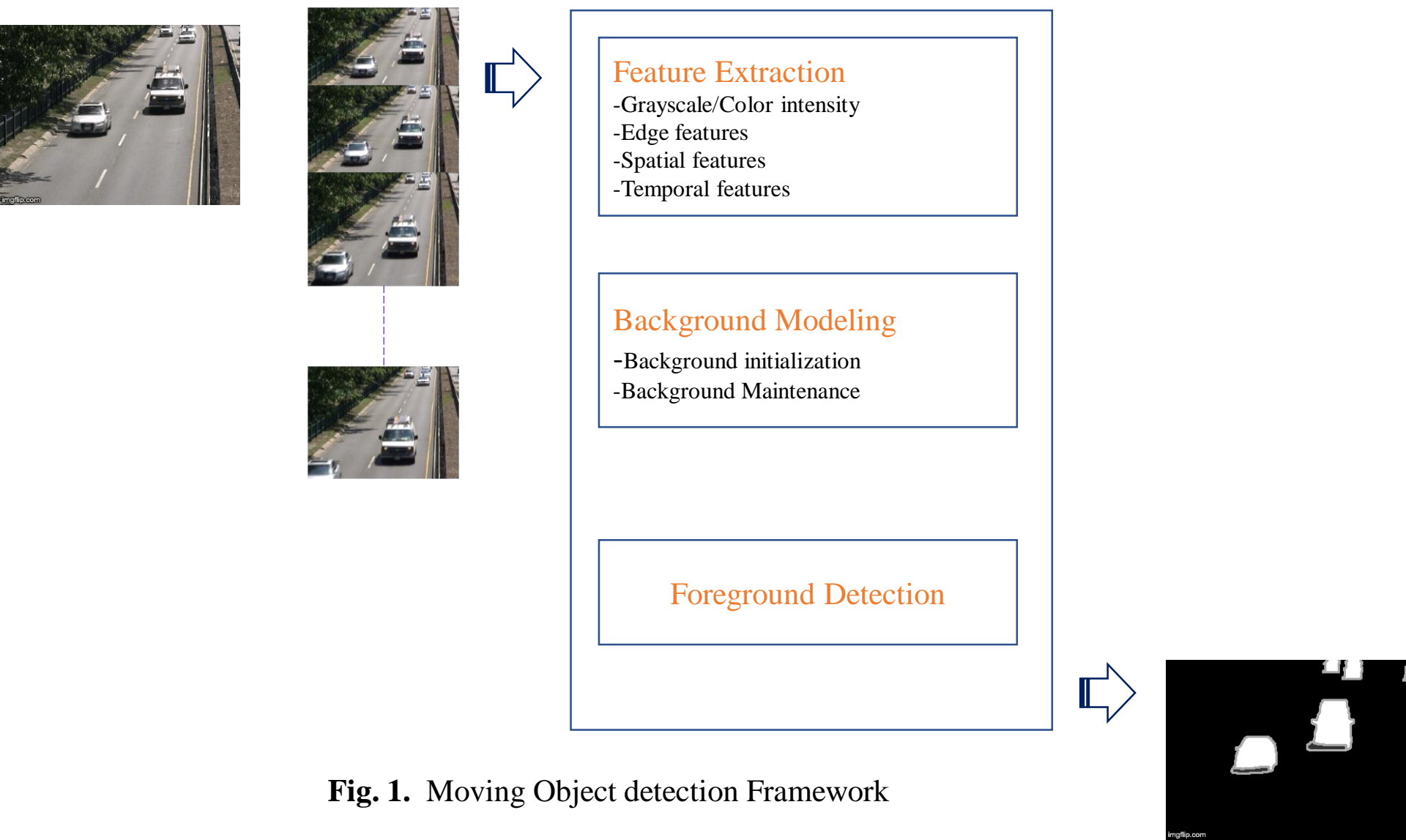


Fig. 1. Moving Object detection Framework

ANTIC

- Paper Title: *ANTIC: ANTithetic Isomeric Cluster Patterns for Image Retrieval and Change Detection*

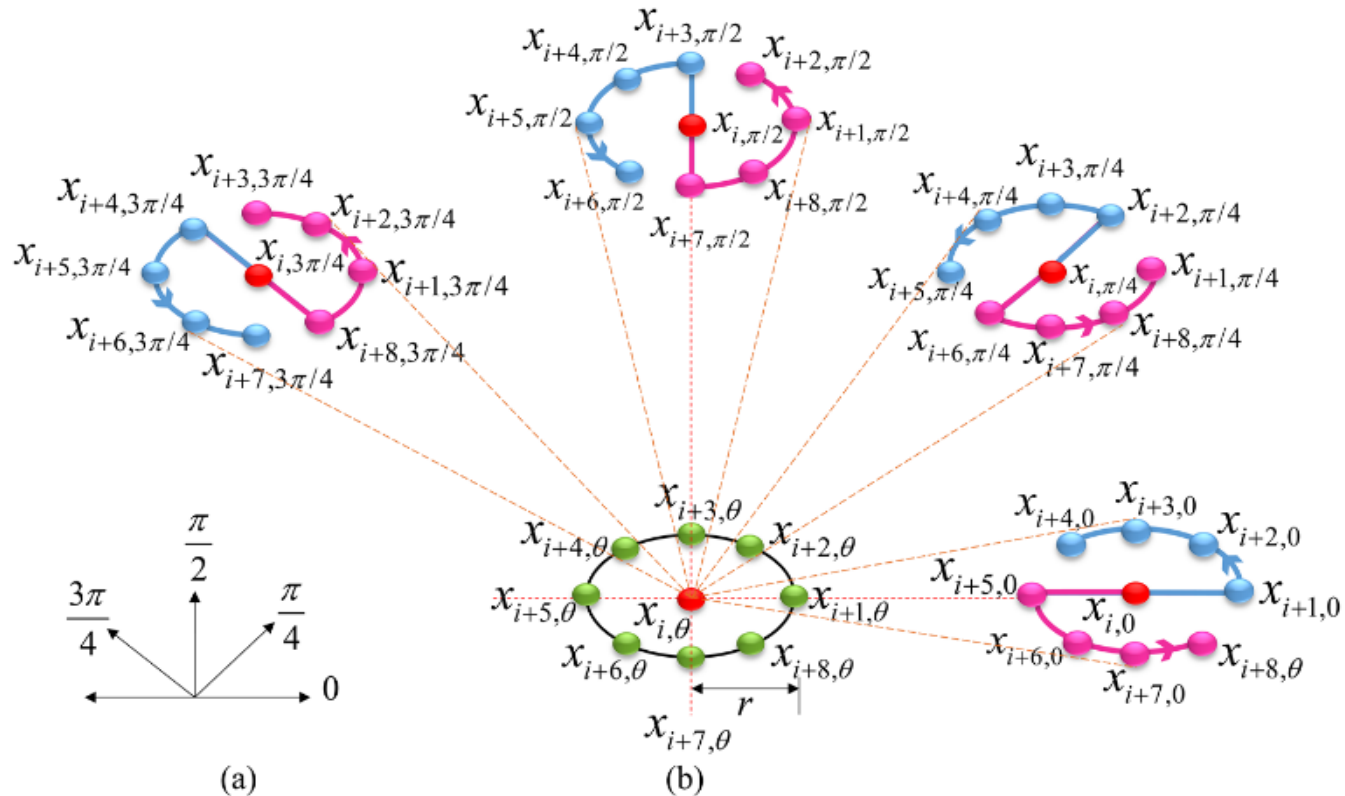


Fig. 2. The Proposed ANTIC descriptor

ANTIC

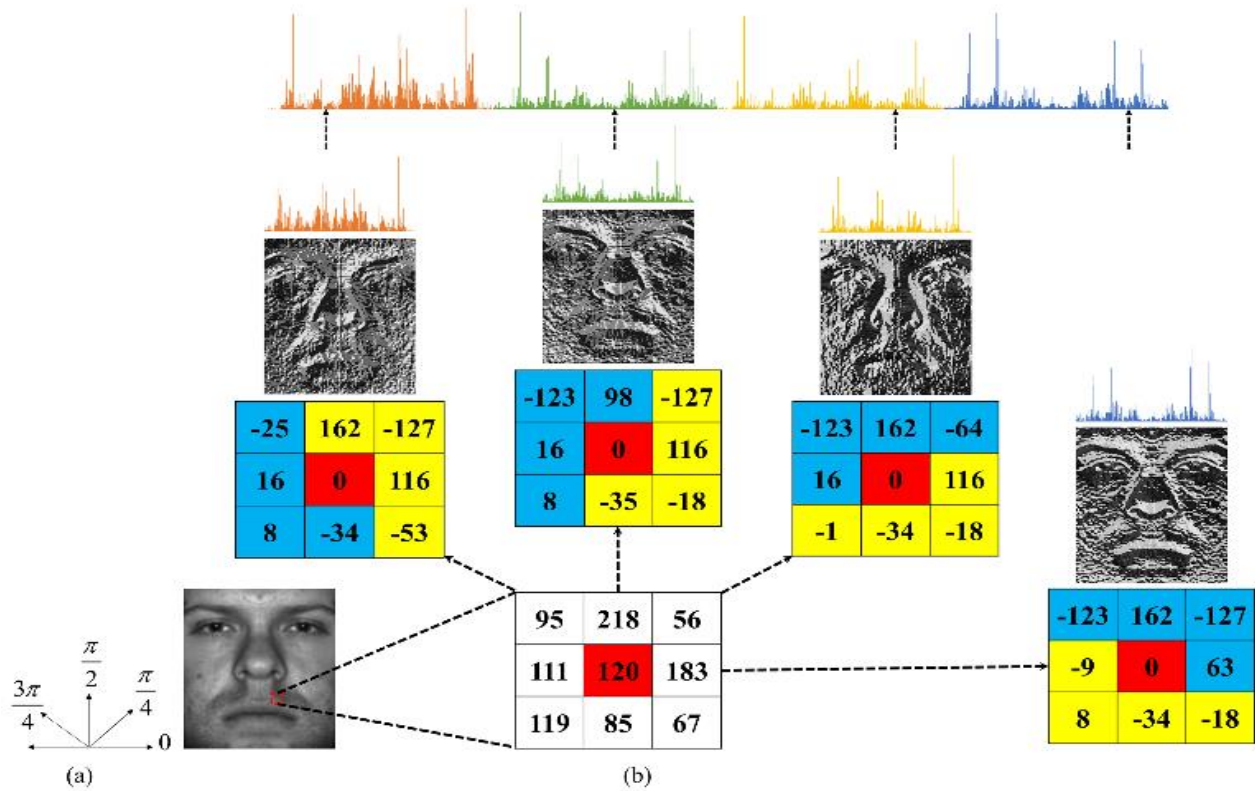


Fig. 3. Illustration of ANTIC feature Extraction System

ANTIC

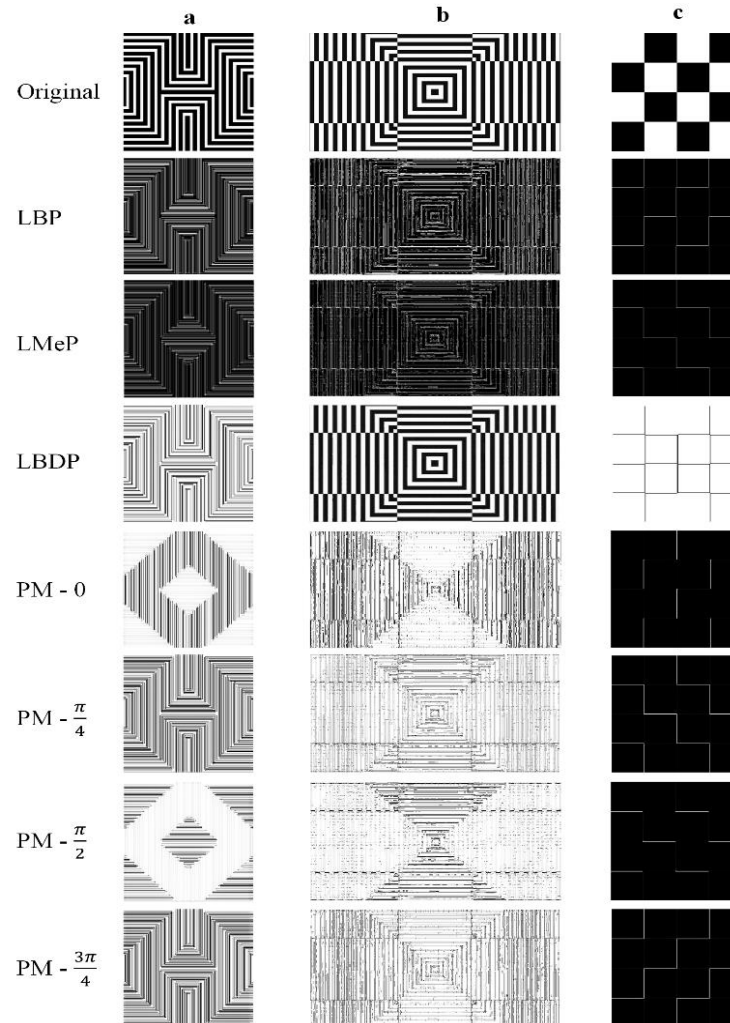


Fig. 4. The comparative analysis of the proposed descriptor along various directions with LBP, LMeP and LBDP feature descriptor

ANTIC

- One of the challenging task in change detection is to make appropriate distinction between the properties of background models and foreground pixels.
- Primarily, the pixel intensities are used to solve this problem but it fails to handle the noise and illumination variations.
- Local descriptors have proven to be very discriminative and are invariant to illumination changes.
- Furthermore, to detect the changes in a video stream, we encoded both the spatial and temporal feature space.

State-of-the-art	Properties
ViBe [2] (2011)	<ul style="list-style-type: none"> • The authors proposed three important background model update strategies: random sample replacement, memoryless update policy, spatial diffusion via background sample propagation. • They further used a constant threshold and static update rate for foreground detection and background model maintenance
PBAS [3] (2012)	<ul style="list-style-type: none"> • The authors introduced dynamic controllers to update the per-pixel decision thresholds and learning rates.
SuBSENSE [4] (2015)	<ul style="list-style-type: none"> • The SuBSENSE computes the pixel-level spatiotemporal feature descriptor LBSP [4], color channel intensity and incorporates the adaptive feedback information to perform background subtraction. • The adaptive feedback mechanism continuously monitors the model fidelity and segmentation entropy to update the decision thresholds, learning rates and background samples.

Proposed Method: ANTIC

- The spatial features (intra-ANTIC) are computed for the background models and the spatiotemporal features (inter-ANTIC) are extracted between the background and current frame.
- These features are extracted by using proximity threshold. This increases the adaptability of the proposed descriptors in challenging visual scenarios.
- The proximity threshold is applied over magnitude variations in the local neighborhood.

Intra-ANTIC

Let I_t be a frame of size $M \times N$ in a video stream $\{I_t\}_{t=1}^V$. The pixel coordinates of image I_t is represented as $I_t(a, b) \forall (a \in [1, M], b \in [1, N])$ and V is the length of the video. Then the intra-ANTIC for an image is computed using

$$\text{intraANTIC}(a, b) = \bigoplus_{i=1}^p D_t(x_{t,u}, x_{t,i}, x_{t, \text{mod}(i,p)+1})$$

$$D(z_1, z_2, z_3) = \begin{cases} 00, & \text{if } |z_2 - z_1| > \tau.z_1 \ \& \ |z_3 - z_2| > \tau.z_1 \\ 01, & \text{if } |z_2 - z_1| > \tau.z_1 \ \& \ |z_3 - z_2| \leq \tau.z_1 \\ 10, & \text{if } |z_2 - z_1| \leq \tau.z_1 \ \& \ |z_3 - z_2| > \tau.z_1 \\ 11, & \text{if } |z_2 - z_1| \leq \tau.z_1 \ \& \ |z_3 - z_2| \leq \tau.z_1 \end{cases}$$

where $u = 0$ and τ is the proximity threshold factor which determines the degree of proximity between two pixels. This value is bound to $[0, 1]$.

Inter-ANTIC

The inter-ANTIC between two frames can be computed using

$$\text{inter}ANTIC(a, b) = \bigoplus_{i=1}^p D(x_{t-1,u}, x_{t-1,i}, x_{t, \text{mod}(i,p)+1})$$

$$D(z_1, z_2, z_3) = \begin{cases} 00, & \text{if } |z_2 - z_1| > \tau.z_1 \ \& \ |z_3 - z_2| > \tau.z_1 \\ 01, & \text{if } |z_2 - z_1| > \tau.z_1 \ \& \ |z_3 - z_2| \leq \tau.z_1 \\ 10, & \text{if } |z_2 - z_1| \leq \tau.z_1 \ \& \ |z_3 - z_2| > \tau.z_1 \\ 11, & \text{if } |z_2 - z_1| \leq \tau.z_1 \ \& \ |z_3 - z_2| \leq \tau.z_1 \end{cases}$$

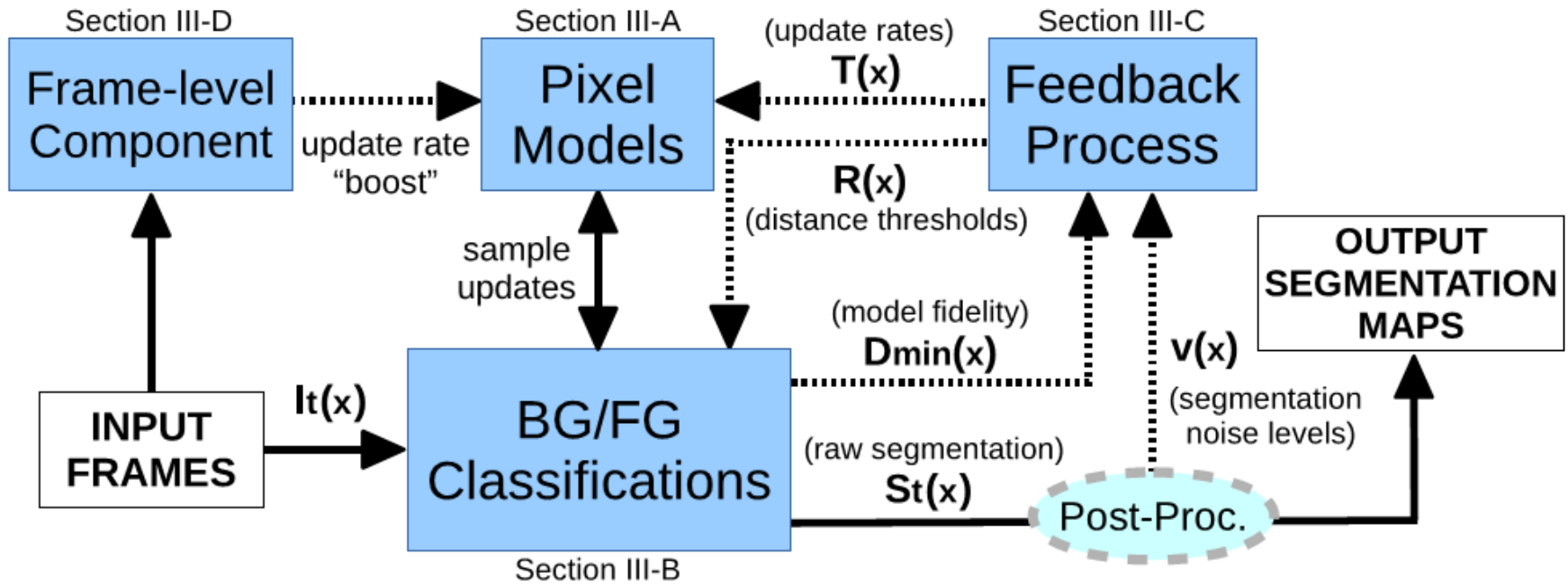


Fig. 5. Block diagram of SuBSENSE; dotted lines indicate feedback relations.

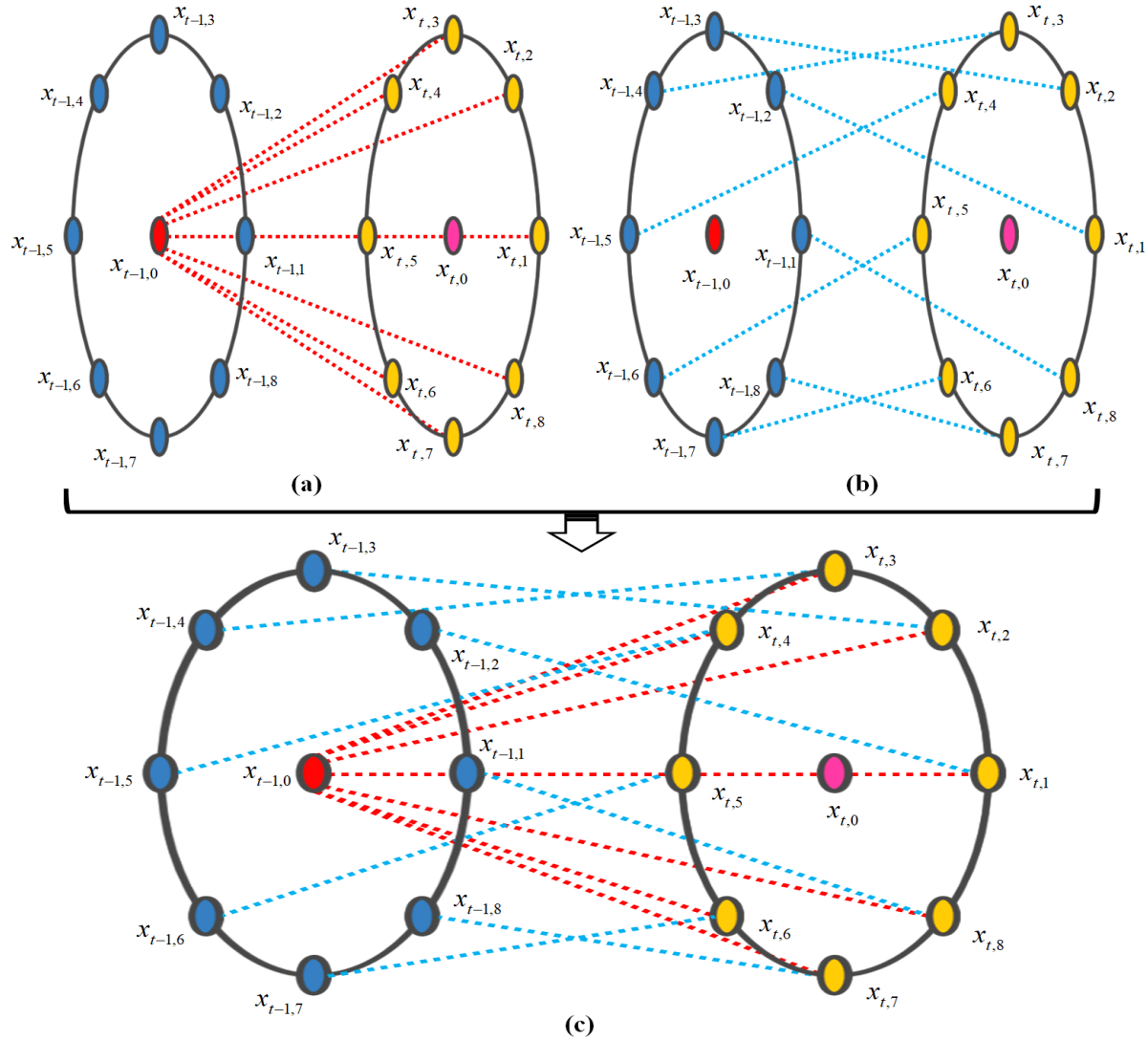
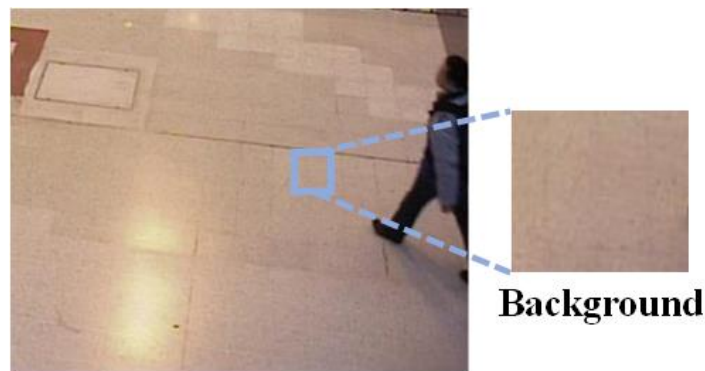
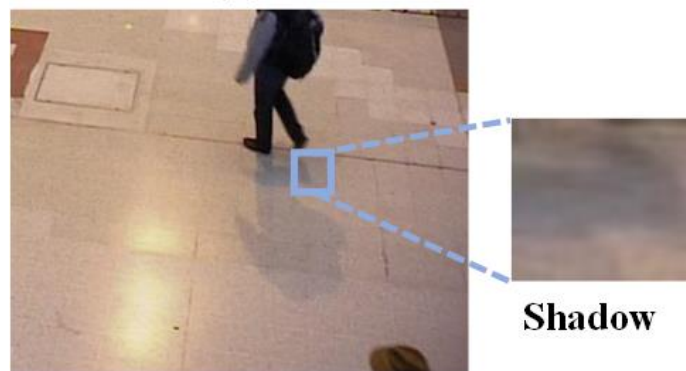


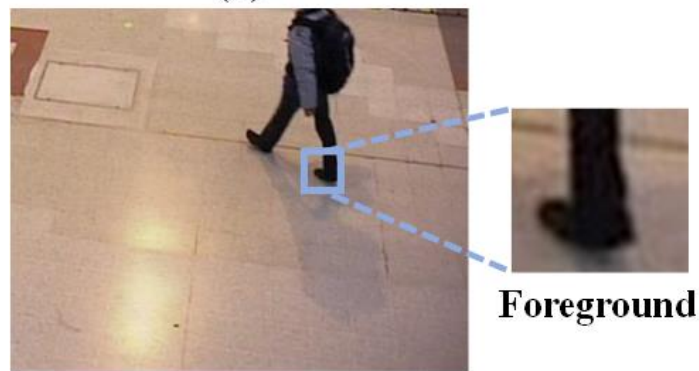
Fig. 6. The inter-ANTIC feature descriptor



Intra-ANTIC
Background reference



Inter-ANTIC
Hamming distance = 2
(Background)



Inter-ANTIC
Hamming distance = 8
(Foreground)

Fig. 7. Demonstrating the effectiveness of intra-ANTIC and inter-ANTIC patterns in video containing shadows

ANTIC: Background Subtraction

- We proposed to use nonparametric background models for background subtraction.
- The pixel-level background model is characterized by the combination of color and intra-ANTIC bit-stream for each color channel.
- The background model can be represented using

$$BM(a, b) = \{s_i(a, b)\}_{i=1}^Q$$

where $s_i(a, b)$ is the background sample at index position i and Q is the total no. of samples.

ANTIC: Background Subtraction

- The similarity matching is performed to identify salient object motions based on hamming distance between the intra-ANTIC and interANTIC bit-patterns.
- If the distance is less than the given threshold, then the current pixel is considered similar to a background.
- This two-step verification technique ensures robust classification of a pixel to become foreground.

ANTIC: Background Subtraction

- At each step, the matching is performed using

$$SM_t(a, b) = \begin{cases} 0, & \text{if } \Xi_t(a, b) < \#_{\min} \\ 1, & \text{otherwise} \end{cases}$$

where $\#_{\min}$ is the minimum number of matches required to label a pixel as background. In our experiments, we set the parameter $\#_{\min} = 2$. The $\Xi_t(a, b)$ can be computed through

$$\Xi_t(a, b) = \#\{DB_{t,i}(a, b) < R_t(a, b), \forall Q\}_i$$

$$DB_t(a, b) = \{\text{dist}(I_t(a, b), BM_i(a, b))\}_{i=1}^Q$$

where $R_t \in \{R_{color}, R_{antic}\}$ are the distance thresholds for intensity and ANTIC respectively.

ANTIC: Model Update

- Furthermore, we update the background models using a stochastic approach as given in ViBe.
- For each pixel classified as background, a randomly selected sample of $B(a, b)$ is replaced by current observation $I(a, b)$ with probability of $1/T$ where T is the model update rate.

ANTIC: Model Update

- Moreover, the randomly selected neighbor of $\text{BM}(a, b)$ is also replaced by the current value with the probability of $1/T$.
- The model update rate T regulates the speed of background model adaptation.
- Large value of T leads to low update probability (thus, no or minimal changes in the model) and vice-versa.

ANTIC: Model Update

- In this paper, we use pixel-level adaptive distance thresholds (R_{color} & R_{antic}) and model update rate (T)
- These parameters are continuously updated by monitoring the background model and feedback scheme.
- In this paper, the feedback scheme requires initial color threshold as 30 and initial ANTIC distance threshold as 3 for adaptive threshold generation.

ANTIC: Model Parameters

- We use the following parameters values: $Q=50, \tau = 0.5$
- Initial color threshold ($R_{\text{color}}=30$) and initial ANTIC distance threshold ($R_{\text{antic}}=3$) for adaptive threshold generation. The remaining parameter values for the feedback scheme are assigned as given in SuBSENSE.
- Furthermore, we use simple post-processing techniques. (median filter & morphological operations) in all the experiments for change detection.



Fig. 8. Foreground detection results of the proposed method and other state-of-the-art methods

Performance Metrics

- Pixel-based Evaluation Metrics

$$Precision = \frac{TP}{TP + FP}$$

$$Recall = \frac{TP}{TP + FN}$$

$$F\text{-score} = \frac{2 * Precision * Recall}{Precision + Recall}$$

$$Specificity(Sp) = \frac{TN}{(FN + FP)}$$

$$PWC = \frac{100 * (FN + FP)}{(TP + FN + FP + TN)}$$

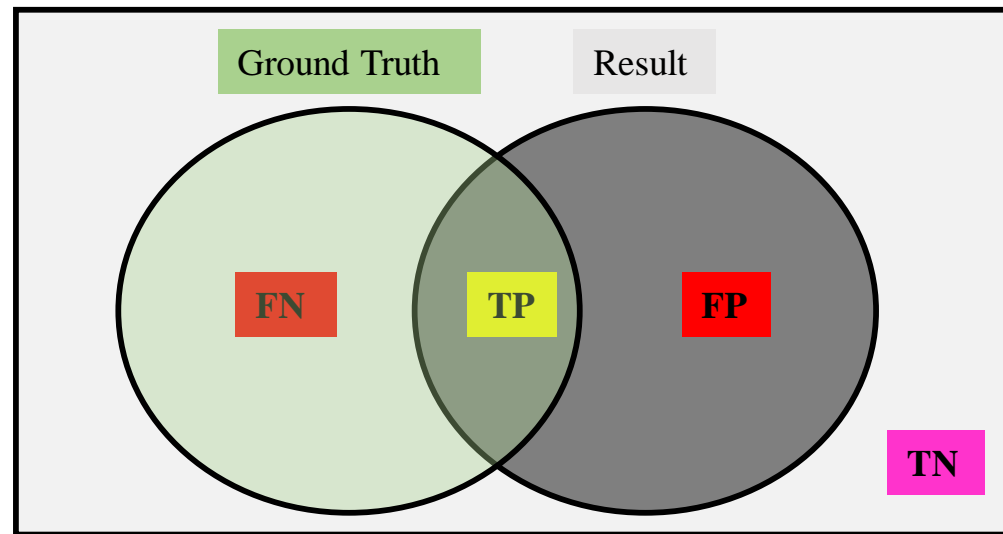


Fig. 9. Pixel based performance evaluation

Table 1 Complete results of the proposed method over twenty-two challenging videos from CDNet 2014 dataset

Video*	Pr	Re	F-Score	Sp	FPR	FNR	PWC
bliz	0.97	0.73	0.83	0.9997	0.0003	0.0031	0.34
skat	0.98	0.88	0.93	0.9993	0.0007	0.0062	0.66
wetS	0.86	0.78	0.82	0.9984	0.0016	0.0029	0.44
P6	0.92	0.95	0.93	0.9989	0.0011	0.0007	0.18
high	0.94	0.94	0.94	0.9959	0.0041	0.0035	0.72
off	0.98	0.92	0.95	0.9988	0.0012	0.0061	0.68
peds	0.97	0.96	0.96	0.9997	0.0003	0.0004	0.07
boat	0.93	0.50	0.65	0.9998	0.0003	0.0031	0.34
can	0.99	0.82	0.90	0.9998	0.0002	0.0065	0.64
fall	0.88	0.90	0.89	0.9978	0.0022	0.0019	0.40
f01	0.74	0.72	0.73	0.9998	0.0002	0.0002	0.05
f02	0.99	0.85	0.92	1.0000	0.0000	0.0003	0.03
sofa	0.86	0.71	0.78	0.9946	0.0054	0.0131	1.77
stL	1.00	0.95	0.98	1.0000	0.0000	0.0024	0.24
tst	0.95	0.35	0.50	0.9963	0.0037	0.1458	12.00
wD	0.30	0.63	0.41	0.9887	0.0113	0.0029	1.40
tmS	0.60	0.86	0.71	0.9840	0.0160	0.0039	1.93
wS	0.30	0.61	0.40	0.9562	0.0438	0.0118	5.40
bac	0.98	0.90	0.94	0.9997	0.0003	0.0020	0.23
Bus	0.80	0.87	0.85	0.9919	0.0081	0.0050	1.06
cpM	0.84	0.95	0.89	0.9832	0.0168	0.0037	1.10
pIn	0.83	1.00	0.90	0.9788	0.0212	0.0001	1.20
Avg	0.85	0.81	0.81	0.99	0.01	0.01	1.40

*bliz: blizzard, skat: skating, wetS: wetSnow, high: highway, off: office, peds: pedestrian, P6: PETS2006, boat: boats, can: canoe, f01: fountain01, f02: fountain02, stL: streetLight, tst: tramStop, wD: winterDriveway, tmS: tramStation, wS: winterStreet, bac: backdoor, bus: busStation, cpM: copyMachine, pIn: peopleInShade

Table 2 The comparative results of the proposed method and other state-of-the-art approaches over twenty-two videos from CDNet 2014 dataset

Method	bliz.	skat.	wetS.	high.	off.	peds.	P6	boat.	can.	fall	f01	f02	sofa	stL.	tmst.	winD.	tmS.	winS.	back	busS.	cpM.	pInS.	Avg.
GMM-G	0.83	0.86	0.61	0.92	0.59	0.95	0.83	0.73	0.88	0.44	0.08	0.80	0.64	0.47	0.45	0.27	0.73	0.41	0.64	0.80	0.64	0.89	0.66
[36]	0.36	1.22	0.98	0.90	4.67	0.09	0.47	0.35	0.82	4.05	1.60	0.09	2.48	3.48	14.67	2.95	1.55	5.49	1.93	1.34	4.16	1.33	2.50
GMM-Z	0.80	0.84	0.56	0.82	0.61	0.92	0.82	0.26	0.64	0.32	0.05	0.58	0.62	0.44	0.37	0.24	0.65	0.41	0.61	0.70	0.64	0.85	0.58
[37]	0.40	1.34	1.02	1.94	4.21	0.16	0.44	1.91	3.02	5.61	1.84	0.23	2.54	3.75	16.25	2.95	1.80	4.14	1.84	1.98	3.93	1.68	2.86
KDE	0.54	0.80	0.12	0.94	0.94	0.96	0.81	0.03	0.18	0.08	0.01	0.19	0.65	0.38	0.23	0.15	0.76	0.40	0.84	0.79	0.86	0.90	0.53
[39]	0.81	2.01	12.32	0.77	0.86	0.08	0.49	35.14	33.19	35.45	13.88	1.72	2.48	4.98	35.70	6.08	1.47	6.25	0.64	1.47	2.05	1.24	9.05
VIBE	0.53	0.71	0.55	0.79	0.72	0.90	0.70	0.22	0.75	0.42	0.09	0.65	0.51	0.70	0.23	0.29	0.62	0.43	0.78	0.67	0.71	0.84	0.58
[40]	0.75	2.95	0.91	2.23	3.04	0.18	0.63	1.61	1.80	3.30	0.76	0.14	2.90	2.25	27.08	2.00	1.95	3.70	0.75	1.92	3.28	1.78	3.00
PBAS	0.82	0.89	0.72	0.90	0.39	0.92	0.72	0.21	0.40	0.89	0.59	0.90	0.53	0.17	0.52	0.47	0.72	0.39	0.97	0.59	0.60	0.89	0.65
[42]	0.38	1.03	0.61	1.15	5.55	0.18	0.70	0.56	2.67	0.40	0.10	0.04	2.96	4.45	11.72	0.69	1.70	3.47	0.13	2.29	4.43	1.34	2.12
LOBSTER	0.47	0.78	0.53	0.89	0.94	0.92	0.93	0.58	0.93	0.25	0.16	0.83	0.71	0.85	0.32	0.27	0.71	0.34	0.92	0.85	0.91	0.89	0.68
[9]	0.81	2.08	0.89	1.23	0.83	0.15	0.18	0.37	0.49	8.90	0.67	0.07	2.02	1.24	23.16	2.64	1.64	8.47	0.30	1.00	1.16	1.28	2.71
SuBSENSE	0.85	0.89	0.80	0.94	0.96	0.95	0.94	0.69	0.79	0.87	0.75	0.94	0.74	0.98	0.50	0.36	0.76	0.45	0.96	0.86	0.93	0.90	0.81
[10]	0.32	0.95	0.46	0.67	0.51	0.09	0.16	0.31	1.22	0.47	0.05	0.02	1.89	0.15	12.10	1.94	1.46	4.82	0.17	1.05	0.95	1.25	1.41
UBSS-1	0.87	0.92	0.56	0.92	0.97	0.96	0.86	0.90	0.93	0.57	0.52	0.92	0.85	0.99	0.89	0.38	0.71	0.46	0.83	0.87	0.87	0.90	0.80
[45]	0.29	0.72	1.53	0.94	0.38	0.08	0.33	0.11	0.44	2.01	0.06	0.03	1.25	0.08	4.48	1.00	1.55	3.51	0.73	1.01	1.76	1.13	1.07
UBSS-0	0.87	0.92	0.48	0.92	0.97	0.96	0.86	0.90	0.93	0.57	0.52	0.92	0.85	0.99	0.63	0.34	0.71	0.46	0.72	0.87	0.87	0.90	0.78
[44]	0.29	0.72	2.05	0.94	0.38	0.08	0.33	0.11	0.44	2.01	0.06	0.03	1.25	0.08	10.03	0.77	1.55	3.51	1.25	1.01	1.76	1.13	1.35
Spec-360	0.78	0.92	0.65	0.94	0.96	0.93	0.90	0.69	0.88	0.90	0.47	0.92	0.79	0.88	0.39	0.15	0.77	0.47	0.97	0.82	0.89	0.90	0.77
[49]	0.43	0.75	0.94	0.68	0.61	0.13	0.29	0.30	0.78	0.37	0.17	0.03	1.63	1.06	14.33	6.83	1.54	5.26	0.12	1.40	1.58	1.25	1.84
IUTIS-1	0.67	0.71	0.55	0.94	0.95	0.97	0.86	0.32	0.41	0.18	0.04	0.74	0.66	0.75	0.25	0.19	0.72	0.44	0.93	0.85	0.89	0.91	0.63
[50]	0.59	3.44	1.32	0.74	0.66	0.06	0.35	2.02	9.90	14.83	3.39	0.14	2.25	1.99	36.51	4.72	1.63	5.22	0.29	1.07	1.49	1.15	4.26
IUTIS-2	0.63	0.89	0.73	0.95	0.48	0.96	0.77	0.59	0.71	0.30	0.07	0.89	0.51	0.30	0.52	0.60	0.74	0.54	0.96	0.71	0.55	0.75	0.64
[50]	0.64	0.95	0.59	0.56	4.86	0.07	0.56	0.48	1.96	7.26	1.98	0.05	2.98	4.10	11.77	0.65	1.62	3.71	0.16	1.76	4.52	2.68	2.45
RMoG	0.61	0.79	0.64	0.87	0.59	0.94	0.75	0.83	0.94	0.67	0.20	0.87	0.55	0.73	0.42	0.43	0.66	0.46	0.78	0.78	0.55	0.77	0.67
[38]	0.66	1.73	0.77	1.47	4.18	0.12	0.60	0.21	0.44	1.23	0.36	0.06	2.83	2.09	13.79	1.08	1.81	5.04	0.96	1.39	4.79	2.49	2.19
SC-SOBS	0.59	0.89	0.51	0.95	0.97	0.95	0.87	0.90	0.95	0.28	0.12	0.89	0.64	0.97	0.84	0.13	0.68	0.43	0.84	0.84	0.57	0.91	0.71
[46]	0.68	1.04	1.23	0.65	0.41	0.10	0.34	0.13	0.34	8.35	0.93	0.05	2.55	0.26	5.98	6.88	1.96	5.51	0.68	1.18	6.71	1.10	2.14
BingWang	0.73	0.89	0.67	0.95	0.79	0.93	0.87	0.85	0.93	0.63	0.77	0.93	0.58	0.98	0.82	0.38	0.64	0.36	0.86	0.85	0.66	0.90	0.77
[67]	0.50	0.97	0.78	0.66	2.53	0.16	0.35	0.19	0.53	1.97	0.04	0.03	2.73	0.19	6.30	1.84	2.01	9.28	0.64	1.06	4.02	1.29	1.73
CP3	0.68	0.90	0.80	0.82	0.96	0.94	0.82	0.54	0.91	0.63	0.17	0.64	0.83	0.80	0.39	0.43	0.74	0.25	0.61	0.75	0.86	0.71	0.69
[65]	1.00	1.00	0.53	2.04	0.50	0.12	0.43	0.87	0.61	1.18	0.61	0.16	1.44	2.30	53.99	0.98	1.52	11.09	2.32	1.81	2.07	3.46	4.09
AAPSA	0.84	0.85	0.69	0.89	0.95	0.96	0.87	0.76	0.89	0.75	0.44	0.36	0.69	0.94	0.47	0.25	0.70	0.41	0.80	0.84	0.76	0.90	0.73
[47]	0.33	1.31	0.64	1.23	0.67	0.07	0.35	0.24	0.72	0.79	0.11	0.71	2.17	0.54	12.55	2.78	1.74	3.88	0.82	1.13	3.87	1.25	1.72
EFiC	0.73	0.92	0.57	0.93	0.95	0.88	0.92	0.36	0.36	0.72	0.23	0.91	0.78	0.98	0.25	0.14	0.79	0.61	0.91	0.80	0.73	0.87	0.70
[63]	0.50	0.74	1.58	0.86	0.75	0.26	0.22	0.53	2.88	1.26	0.47	0.04	1.65	0.17	48.65	7.91	1.29	2.59	0.38	1.68	3.12	1.63	3.60
EFiCv2	0.76	0.90	0.62	0.93	0.93	0.95	0.91	0.37	0.34	0.56	0.27	0.93	0.83	0.98	0.49	0.14	0.79	0.63	0.95	0.86	0.85	0.90	0.72
[64]	0.45	0.94	1.20	0.78	0.95	0.11	0.24	0.50	2.91	2.43	0.37	0.03	1.30	0.24	30.40	7.15	1.28	2.68	0.20	1.10	1.89	1.26	2.66
Graphcut	0.90	0.92	0.87	0.90	0.35	0.93	0.68	0.57	0.12	0.72	0.08	0.91	0.56	0.21	0.50	0.52	0.73	0.45	0.94	0.59	0.58	0.75	0.63
[48]	0.24	0.76	0.31	1.14	5.74	0.15	0.87	0.52	52.01	1.20	1.10	0.04	2.94	4.32	12.01	0.65	1.54	5.62	0.24	2.38	4.49	2.75	4.59
MultSpat	0.71	0.62	0.57	0.87	0.80	0.95	0.75	0.48	0.89	0.41	0.14	0.82	0.60	0.60	0.62	0.21	0.62	0.44	0.85	0.70	0.85	0.86	0.65
[66]	0.52	4.78	0.97	1.45	2.39	0.09	0.66	0.70	0.83	4.27	0.51	0.08	2.64	3.44	20.40	3.02	2.41	5.79	0.55	1.85	2.08	1.65	2.78
PM	0.83	0.93	0.82	0.93	0.95	0.96	0.94	0.65	0.90	0.89	0.73	0.92	0.78	0.98	0.50	0.41	0.71	0.40	0.94	0.85	0.89	0.90	0.81
	0.34	0.66	0.44	0.18	0.72	0.68	0.07	0.34	0.64	0.40	0.05	0.03	1.77	0.24	12.00	1.40	1.93	5.40	0.23	1.06	1.10	1.20	1.40

* The first and second row of every method are the F-Score and PWC measures.

**The references are corresponding to the original ANTIC paper*

References

- [1] Y. Wang, J. Pierre-Marc, P. Fatih, K. Janusz, B. Yannick and I. Prakash. CDnet 2014: an expanded change detection benchmark dataset. In *Proceedings of the IEEE Conference on Computer Vision and Pattern Recognition Workshops*, pages 387-394, 2014.
- [2] O. Barnich and M. Van Droogenbroeck, “ViBe: A universal background subtraction algorithm for video sequences,” *IEEE Trans. Image Process.*, vol. 20, no. 6, pp. 1709–1724, Jun. 2011.
- [3] M. Hofmann, P. Tiefenbacher, and G. Rigoll. Background segmentation with feedback: The pixel-based adaptive segmenter. In *Proc. IEEE Comput. Soc. Conf. Comput. Vis. Pattern Recognit. Workshops*, pages 38–43, Jun. 2012.
- [4] St. Charles, P. Luc, and G. A. Bilodeau. Improving background subtraction using local binary similarity patterns. In *Applications of Computer Vision (WACV), 2014 IEEE Winter Conference on*, pages 509-515, 2014.